

Reply to Referee #2 (Dr. F. Wienhold)

Thank you very much for your reviewing our manuscript and providing us valuable comments and suggestions.

This contribution presents a new lightweight balloon-borne Cloud Particle Sensor (CPS). It describes the instrumental setup with the constraints imposed by the conditions on operational soundings balloons, and explains how particle concentrations is estimated from the primary count rate. Results from test flights are presented that compare two instrumental setups and provide simultaneous measurements with the Cryogenic Frostpoint Hygrometer (CFH). Various midlatitude and tropical cloud layers are probed illustrating the deployment in a wide range of cloud types. This clearly demonstrates that different cloud types (pure water, mixed phase to cirrus) can be well identified and characterized.

The paper is well organized. The current development state of the new sensor and the experience gained in various balloon sounding deployments deserve publication in Atmospheric Measurement Techniques. However, limitations and uncertainties need to be addressed more clearly, and a roadmap for future development should be added.

Thank you very much for your understanding and positive evaluation. Please see below for our answers to your questions.

General comments

The term degree of polarization (DOP) is introduced unconventionally including differently adjusted detector sensitivities leading to an observed range from -1 and 1, whereas in common notion it would be expected to range from 0 to 1. To avoid confusion this needs to be stated more explicitly – see specific comments.

In the revised manuscript, we will add the following explanation on the factory calibration process: The rough-surface particles of 30–40 μm diameter are the spores of the *Lycopodium clavatum* Linnaeus provided by the Association of Powder Process Industry and Engineering (APPIE), Japan. Other rough-surface particles may also work; the key point is that we use certain particles so that we can calibrate the two detectors after the instrument is fully assembled. The sensitivity of the two detectors are differently adjusted so that the calibration particles give zero DOP on average (using 251 particle data). Typically, detector #2 is about three times more sensitive than detector #1; this is

consistent with the fact that the polarization plate used has 34–35 % transmittance.

The air flow speed in the instrument is essential both to convert the count rate into number density, and to correct for signal overlap caused by multiple particle detection. Substantial flow speed reduction with respect to the ascent rate is reported for the instrument geometry used, rough agreement is found only for larger cross sections tested. Equating the flow speed with the typical sounding balloon ascent rate of 5 m/s – with a resulting reference signal width of 1 ms – is inappropriate when the effects number density conversion and overlap correction are not discussed (see also specific comments). Low number density regions near ground in Figures 5 and 7 with signal widths in excess of 1 ms conflict the undiminished flow assumption. The corrected particle count rate should be clearly addressed as an upper bound estimate, not just as corrected value.

First, in the revised manuscript, we will add a new appendix, Appendix B where we will show the results from a CPS with two hot-wire anemometers (with the uncertainty of $+/-1$ m s^{-1} ($k = 2$)) launched at Moriya at 17:11:47 LT on 23 November 2012 (see Figure R1-2). The two hot-wire anemometers were placed within a 6-cm long duct (with a similar inner cross section to that of the CPS's air inlet), near the two openings, and this duct was attached at the bottom side of a CPS. Thus, the anemometer #1 is located \sim 4 cm below the detection area, and the anemometer #2 is 9–10 cm below the detection area. Figure R1-2 compares the balloon ascent rate and the flow speed in the duct measured with two anemometers. From the surface up to \sim 10 km, the balloon ascent rate is 5–6 m s^{-1} , flow speed measured by the anemometer #1 is 4–5 m s^{-1} , and flow speed for #2 is 3–4 m s^{-1} , with increasing discrepancy between #1 and #2 at higher altitudes. Between 10 and 16 km, the balloon ascent rate is \sim 5 m s^{-1} , flow speed for #1 is \sim 4 m s^{-1} , and flow speed for #2 is 1–2 m s^{-1} . It is expected that the actual flow speed for #1 and #2 would not differ because of the same cross section of the air flow. However, the measurement results show that this was not the case. Possible reasons include the horizontal difference in the flow speed within the duct and in the location of the two anemometers (i.e. the anemometer #2 may have been located closer to the duct wall during the flight). Also, these anemometers might have had some directivity dependence, which had not been evaluated in the laboratory experiments. Considering the additional flow of up to 2 m s^{-1} due to the pendulum motions, assumption of a constant flow speed of 5 m s^{-1} with the uncertainty of a factor of \sim 2 (as the contribution from the flow-speed assumption) is not unreasonable.

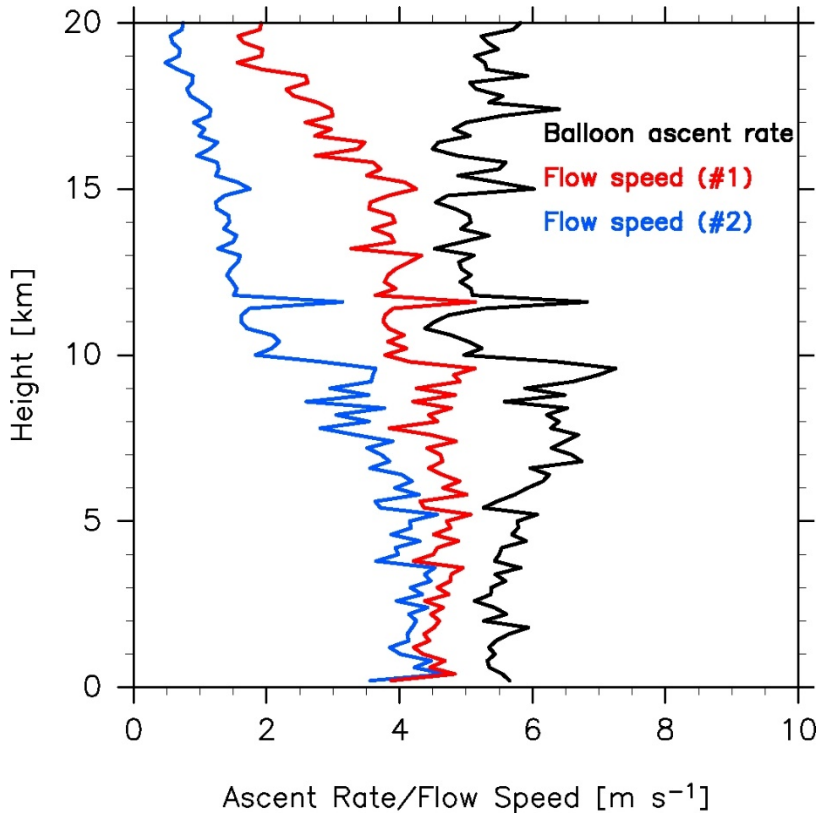


Figure R2-1. Vertical profiles of balloon ascent rate (black) and the flow speed within a duct (with a similar inner cross section to that of the CPS's air inlet) attached to a CPS measured with two hot-wire anemometers, one placed ~ 4 cm below the detection area (#1, red) and the other ~ 10 cm below the detection area (#2, blue). Taken at Moriya, Japan, launched at 17:11:47 LT on 23 November 2012. For all three profiles, 0.2-km averages were taken.

Second, in the revised manuscript we will have a new appendix, Appendix C where we discuss the impact of different flow speeds on the number density conversion and the count number correction (see the next paragraph and Figure R2-2). In this way, the uncertainty in the number concentration values from the CPS is better understood, and the future CPS users can use this information to process and evaluate their data.

Planned Appendix C:

Both the conversion from number of particles N [s^{-1}] to number concentration C [cm^{-3}] and the correction factor for N depend on the flow speed within the detection area v [$m s^{-1}$]. As the cross section of the detection area is $\sim 1 cm^2$, C is given by $N/(100v)$. As the vertical extent of the detection area is ~ 0.5 cm, the correction factor for N (see discussion in Sect. 2.3) is $4 \times (psw/(5/v))^3$ if psw is greater than $5/v$, where psw is particle signal width in ms; if psw is smaller than $5/v$, the correction factor is unity. Figure C1 shows the relationships between N and C and between psw and the correction

factor for $v = 3, 5$, and 7 m s^{-1} . This indicates the contribution of the uncertainty in v (see also Appendix B) to the uncertainty in (corrected) N .

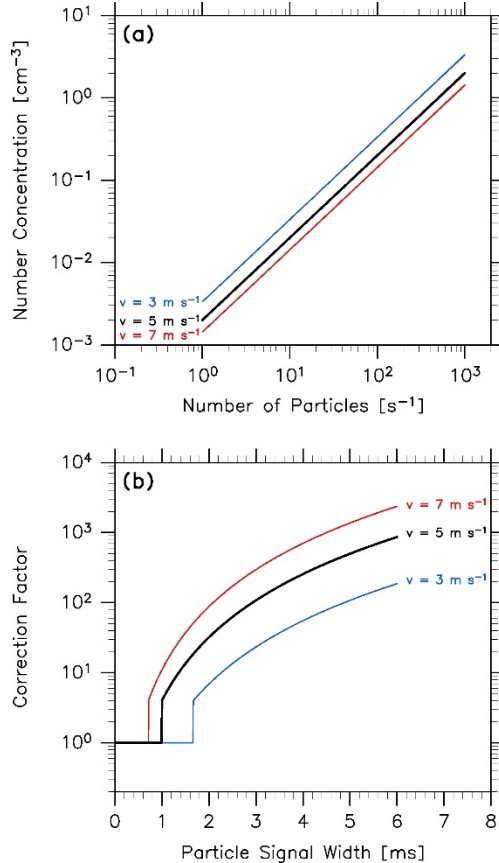


Figure R2-2. (Planned Figure C1.) Dependence on the flow speed within the detection area (v in m s^{-1}) for (a) the conversion from number of particles in s^{-1} to number concentration in cm^{-3} and (b) the correction factor for the number of particles (N in s^{-1}) with respect to the particle signal width values in ms. Shown are for 5 m s^{-1} (black), 3 m s^{-1} (blue), and 7 m s^{-1} (red).

Finally, are the “Low number density regions near ground in Figures 5 and 7 with signal widths in excess of 1 ms” the surface to $\sim 500 \text{ m}$ region where the signal width is sometimes $\sim 1.5 \text{ ms}$ for Figure 5 and $\sim 1.1 \text{ ms}$ or $\sim 3 \text{ ms}$ for Figure 7? Yes, this indicates that the assumption of 5 m s^{-1} is sometimes not valid. We will more clearly write that the corrected particle count rate should be regarded as an upper bound estimate, not just as corrected value.

The Meisei radiosonde interface is limited to 25 bytes/s while other radiosonde offer much larger bandwidth as 80 bytes/s for the Internet Systems iMet or 100 bytes/s for Vaisala RS41. These would

allow addressing the above problem by a better characterization of the signal width distribution instead of just transmitting the first six samples. I suggest adding a perspective for future development which could include real-time (onboard) data processing options in conjunction with increased downlink capacity. This could illustrate how the promising potential of this sensor could be exploited further.

Thank you very much for your suggestions. We assume that both iMet and RS41 radiosondes support the XDATA protocol. The authors from Meisei will consider to work with other researchers to develop a processing and interfacing board for these and other radiosondes.

Specific comments

Page 1, line 22: before “of the instrument”, replace “volume of the detection area” by “ascent rate together with the detection volume and exposed cross section”.

The number 2 cm^{-3} is a multiplicative inverse of the volume of the detection area (0.5 cm^3). If there is more than one particle in the detection area, a count loss would occur.

Page 3, lines 3-13: A very approximate cost might be indicated here.

For the first commercial version, the price is about 4–5 times of that of the modern radiosondes.

Page 3, line 12: The situations covered by the four test flights could be mentioned here.

We will do so.

Page 3, lines 16 to 27: The orientation of the rectangular slits should be indicated explicitly in the text or the related Figure 1.

We will revise the relevant sentence as:

The slit in front of the light source is 0.55 cm (parallel to Figure 1, i.e. the space shown in Figure 1) \times 1.0 cm (perpendicular to Figure 1), while the slits in front of the two detectors are 0.50 cm (parallel) \times 1.0 cm (perpendicular).

Please also see Figure R1-4 in the Reply to Referee #1.

Pages 3, line 30: do the “rough-surface particles” cause full depolarization and thus about equal sensitivity for both channels, or is the cross-polarized detector tuned more sensitive due to calibrating with only partially depolarized light?

Yes for both. Please see the answer to the first general comment.

Page 4, lines 6, 7: replace “gives” by “determines”, and “other factors” by “polarization”.

Will be replaced.

Page 4, line 15 (compare comment p 3, l 30): To not confuse the reader it should be stated that for equally sensitive detector the DOP should be between 0 and 1. As detector #1 senses the sum of co- and cross-polarized scattered light, negative DOP values can only result from higher sensitivity of detector #2.

Thank you very much for this suggestion. Please see the answer to the first general comment.

Page 4, line 16: mentioning “the uncertainty in the factory calibration”: Is there clear calibration target?

Please see the answer to the first general comment.

Page 4 line 20: Replace “various” by “nonzero”.

“Various” is correct. Please see the answer to the first general comment.

Page 4, lines 26, 27: It should be stated that particle overlap excludes flow rate determination: the two signal-width interpretations are complementary.

Yes, we will add this point.

Page 5, line 12: Replace “is 1.0 cm longer” by “extends 1.0 cm”.

Will be replaced.

Page 5, line 19: Other radiosondes offering external instrument interfaces provide higher bandwidth, e. g. 80 bytes/s (Intermet iMet-IRS) or 100 bytes/s (Vaisala RS41). This additional capacity could be used in the future development perspective.

We will add this point as a possibility.

Page 6, line 10: The experimental findings described in this section confirm that the flow rate through the instrument is reduced, as expected. With the tested larger cross section the flow agrees with the ascent rate, but for the configuration used in what follows it is only about half the balloon ascent rate. It should be stated that assuming the nominal flow speed of 5 m/s implies under-estimating both the count rate and the 1 ms reference signal width.

Please see the answer to the second general comment. Note that if the actual flow speed was e.g. 3 m s⁻¹, the threshold signal width should be 1.67 ms; thus, assuming 5 m s⁻¹ for this case would result in overestimation of the correction factor f and the corrected count rate.

Page 6, line 27: The signal width factor f enters the count rate correction to the third power. An assessment of the consequences should be provided.

As explained in the answer to the second general comment, we will include the information on the quantitative consequences of this treatment.

Page 7, line 5: Replace “is close or even greater” by “exceeds”, and delete “highly” in line 6: Ice saturation between 120% and 130% are frequently observed without cloud formation.

Will be replaced.

Page 8, line 10: Description of future work could be anchored here which allows for an improved signal width characterization rather than just sending the first six samples.

We will describe this possibility here and in Section 4.

Page 8 line 11: Not calculating the DOP for signals exceeding 7 V contradicts the statement on page 4, lines 17 to 22.

We did not calculate the DOP for signals exceeding 7 V because a strong peak appears at zero DOP

for “ice” particle cases, while the main message on page 4, lines 17 to 22 was that larger “spherical” (and thus water) particles might still give a DOP distribution for spherical particles (please also see Figure R1-1 in the Reply to Referee #1). In practice, all the flight cases shown in the paper did not detect “water” particles with signals exceeding 7 V (Figs. 3c, 3i, 5c, (7c), and 8c), while they detected “ice” particles with signals exceeding 7 V. Therefore, there is no contradiction. However, we will add more explanation here so that the readers would not be confused.

Page 9, line 24: What is the major difference of “the first commercial version” flown 2015 versus the instrument launched 2013? Near ground level signal width of Figure 5 appears to have increased with respect to Figure 3.

The major difference is in the Styrofoam flight box. In and before 2014, it was made by hand. Also, the length of the inlet duct is slightly different. Thus, there should be no difference in quality in the signal width data. The difference between Figures 3 and 5 near the ground is considered to be due to the actual difference in the nature of the particles. For the case of Figure 3, please see also the discussion with Referee #3.

Page 10, line 3: Excluding DOP analysis again contradicts page 4, lines 17 to 22.

Please see above. We will add more explanation so that the readers would not be confused.

Page 10, lines 10-11 and 31: The authors set a (debatable) signal width limit of 1 ms as onset for particle overlap correction (see p 6, l 24). This should be reflected using 1 instead of 0 as lower limit in the ranges given for the signal width.

For all the current figures, we set the lower limit as -1.0, to clearly show all the data points. As in the answer to the second general comment (Figure R2-2), we will address the issue of the choice of signal width threshold in a different way.

Page 10 line 33: “for some reason” needs further specification: instrumental or telemetry failure?

Probably, this is related to the CPS board or the interface board, but there also is a possibility of telemetry failure.

Page 11, line 15: See signal width range comment for page 10.

Please see above.

Page 11, lines 16-20: Supersaturated layers above cirrus cloud tops are not surprising and have been discussed in detail in Brabec et al. (2012), including microphysical modeling.

Thank you for pointing to the paper by Brabec et al. for the supersaturation issue. We will cite this paper again here.

Page 11, line 21: Which of the lidar wavelengths mentioned is used for analysis and displayed in Figure 10?

The backscattering coefficient is at 1064 nm, and the depolarization ratio is at 532 nm. We will add this information in the revised manuscript.

Thank you very much again for your comments and suggestions. Please also see the discussion with the other two referees.